NanoNEXT

Research Article

DOI: 10.54392/nnxt2543

Real Time Pesticide Contaminant Monitoring Using Hybrid Mxene Doped Graphene FET Biosensors in Surface and ground Water

Devaraj Somasundaram [a,*], Usha Chauhan [a], Sivakumar Poruran [b], Chandrasekar Sivakumar [c]

[a] Department of Electrical Electronics and Communication Engineering, Galgotias University, Greater Noida, India
[b] School of Electronics and Communication Engineering, Dr NGP institute of Technology, Coimbatore, India
[c] Research Center for Materials Nano architectonics (MANA), National Institute for Materials Science (NIMS), Tsukuba 305-0044, Japan.
* Corresponding author Email: somgce@gmail.com
DOI: https://doi.org/10.54392/nnxt2543
Received: 13-06-2025; Revised: 23-11-2025; Accepted: 05-12-2025; Published: 12-12-2025

Abstract: In many parts of the world, pollution caused by chemical releases into water systems has put aquatic ecosystems and human health at risk. Storm water overflows, industrial, agricultural, and wastewater treatment facilities are some of the sources of chemical discharge. It is crucial to develop and implement quick, dependable, and sensitive analytical detection technologies in order to meet these limits. The development of electrochemical biosensors for environmental toxicants, such as pesticides and heavy metals, has advanced over the last few decades. In this paper, a novel Mxene doped graphene FET is proposed to detect the pesticide and contaminations in water. This sensor is electronically compactable and has high chemical sensitivity. Due to the lack of an efficient method for distinguishing defective devices from preselected uniform devices based solely on electronic properties, two-dimensional (2D) electronic sensors frequently experience device-to-device variations. This causes sensor inaccuracy and slows down the real-world applications of the sensors. Real-time spontaneous detection of pesticides such as atrazine and metolachlor in flowing tap water was made possible by our sensors. In order to maximise the potential of electronic sensors for tracking contaminants in flowing water, this work provides a dependable quality control procedure.

Keywords: MXene, Graphene, FET Biosensor, Microfluidic System, Pesticide Detection, Water Monitoring

1. Introduction

Although pollution from human activities has affected aquatic biodiversity and made water more scarce, water is nevertheless necessary for life on Earth. Some chemicals pose a risk to humans, animals, and aquatic plants, despite the fact that they are necessary for daily life. Water treatment facilities, home and industrial discharge, agriculture, and air (via rain and dust) [1] are some of the sources of entry into surface waters. This list includes pesticides, dioxin and chemicals similar to it, heavy metals, polyaromatic hydrocarbons (PAHs), endocrine disruptor compounds (EDCs), chloroalkanes, and polybrominated biphenyl ethers (pBDEs) [2, 3]. Surface water that has quantities of these pollutants below the EQS limits specified by these directives is said to have good chemical status.

The Drinking Water Rules in India have strict limitations on pesticides in drinking water. A single pesticide's limit is 0.1µg/L, while the total number of pesticides discovered and measured throughout the monitoring method is 0.5µg/L. Apart from older mines and contaminated industrial/waste sites that can lead to contamination with As, Pb, Cu diffuse sources of pollution from agriculture (nitrates and pesticides) continue to be a problem for groundwater. Controlling the concentration of dangerous chemical parameters is necessary to guarantee the safety of the water [4, 5]. The World Health Organisation (WHO) has been creating and revising guidelines for all water quality criteria continuously since 1983. When formulating legislation pertaining to water quality, national and regional governing bodies use these as a basis. The levels recommended by the WHO allow for a safe lifetime of consumption while accounting for the possibility that some chemicals may be ingested through food or other sources (such as inhalation) [6-8]. However, due to societal, economic, and environmental considerations (such as the amount of

water drunk daily or high background concentrations), these values may deviate from local targets.

The best kind of sensors for water quality monitoring are those that don't require much upkeep and can run continuously, independently, and without the need for chemicals. Solid state sensors have become a common type of sensors for this purpose, including electrical and electrochemical sensors. Two types of electrical sensors that detect changes in a transducing material's conductance are field-effect transistors (FETs) and chemiresistive sensors [9, 10]. Graphene-based materials are ideally suited to be the transducers in this kind of sensor due to their remarkable electron transport characteristics and simple functionalization. Compared to thin metal films, 2D materials—such as graphene with metal carbides (MXenes), and metal dichalcogenides (TMDs)—have lower sheet resistance and superior surface chemical sensitivity because they are one to a few atoms thin [11]. A thick, single-layer, planar, two-dimensional [12, 13] carbon crystalline allotrope is called graphene.

It serves as the foundation for one of the most significant allotropes of carbon-graphite, as well as fullerenes, carbon nano tubes, charcoal, and other substances. The constituents of graphene are carbon atoms that have undergone sp2 hybridization and are joined to create extended benzene ring structures. Owing to this configuration, graphene is recognised for its exceptional electrical characteristics, demonstrating electron mobility as high as 250,000 $cm^2 V^{-1} s^{-1}$. The hydrophobic characteristic of graphene makes standard Atomic Layer Deposition (ALD) unfeasible for the deposition of dielectric on graphene layers [14]. Consequently, the graphene surface is typically functionalized using NO_2, O_3, or other substances to enable the deposition of dielectric material on top of it. However, utilising graphene is defeated [15, 16] because this strategy typically causes a significant loss in the layer's mobility. It has also been demonstrated that the mobility of electrons and holes can be reduced by up to 85% when SiO_2 is used as the gate dielectric.

A novel class of 2D materials called MXenes combines metallic conductivity with a hydrophilic surface. MXene may be a good option to develop biologically friendly [17] field-effect transistors (FET) for quick, simple, and label-free biological event detection due to its hydrophilic surface feature and 2D layered atomic structures. MXenes are notable for their ease of micromachining to fit a wide range of shapes with sizable contact surfaces. This characteristic can considerably reduce the complexity of device manufacturing methods, which would normally call for intricate operations like chemical vapour deposition, mechanical exfoliation, or epitaxial growth.

These techniques, which can be expensive or low-yield, have been used to FET devices made of graphene, carbon nanotubes, nanowires, and other materials. Many FETs with the graphene and the other materials were discussed earlier with their specific electrical and characteristics properties. In this manuscript a hybrid graphene and MXene integrated biosensor is proposed to detect the pesticide and heavy metals in the water.

2. Materials and Methods

2.1 Fabrication Process

The fabrication of the Mxene and graphene based FET sensor involves many layers to layer diffusion process as shown in figure 1. The process of fabricating a device begins with its design and proceeds through one or two stages of metal deposition, lift-off, high-k atomic layer deposition, and e-beam lithography, each of which we will briefly describe in this section. Steps in the process are schematically depicted. Because of its random character, exfoliated Mxene and graphene generated by EBL is unavoidable during the manufacturing of MGFETs. E-beam lithography is used in one stage for back-gated devices and two steps for top-gated devices. The Raith Turnkey 150 SEM and E-beam lithography system exposed PMMA that was roughly 210 nm in diameter and spun as an EBL resist. Methyl isobutyl ketene (MIBK) formed the resist, and then isopropanol (IPA).

Ti and Au are deposited using electron beam physical vapour deposition (PVD) at a thickness of 10/50 nm. Ti is utilised to address the gold adhesion issue on SiO_2. Following lift-off in acetone and a brief sonication phase, the source and drain connections are illustrated in Figure. It is possible to improve charge management and screening effect by using a high k material as a gate insulator. To have a high-quality, high-k material with fewer flaws in the graphene sheet, the deposition technique is essential. On graphene and Mxene, atomic layer deposition (ALD) is recognised as a suitable option for high-k deposition. A process of chemical vapour deposition known as atomic layer deposition (ALD) is thought to use sequential self-terminating gas-solid interactions. For an ALD tool to create a cycle, four steps must occur in the chamber/reactor.

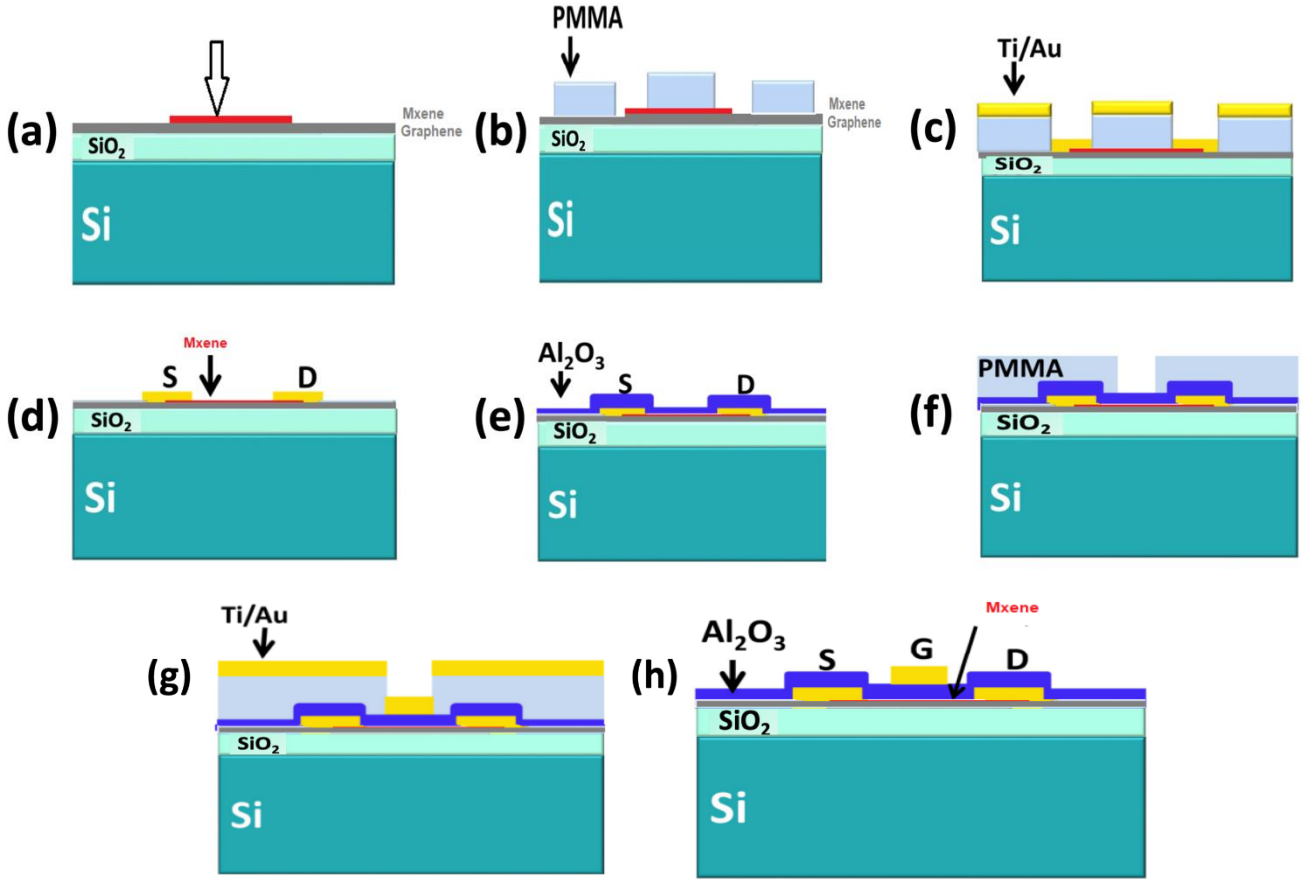

Figure 1. Fabrication process of MGFET

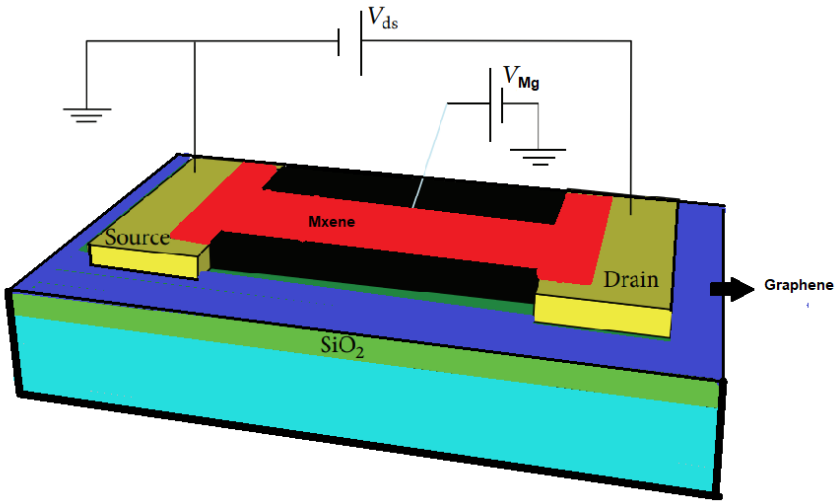

Figure 2. MGFET biosensor

Functional hydroxyl group of the surface reacts with the first reactant gas (trimethylaluminum in the case of Al_2O_3 deposition). After the surface hydroxyl group saturates, the process comes to an end. This stage involves removing the reactor's residual gas (trimethylaluminum) and by-product (methane). To revive the surface, pulse the second reactant, this is water vapour. Upon surface saturation, the process comes to an end. Nobody is inside the reactor. A desirable amount of material is deposited on the surface by repeating this cycle. 6–8 nm, after applying aluminium to the sample using e-beam vapour deposition, it was left to naturally oxidise in the air. After that, the sample was moved to the ALD reactor to undergo annealing and in-situ Al_2O_3 deposition, with

water vapour and trimethylaluminum serving as the reactant gases.

To achieve greater contrast under an optical microscope, Mxene with Graphene was exfoliated from a natural Ti_3C_2 -MXene micro-pattern using graphite and then transferred onto the appropriate Si/SiO_2 substrate with a 99 nm thick oxide layer. To create EBL alignment markings, a cycle of photolithography, tungsten deposition, and lift-off was carried out prior to graphene transfer. Electron beam lithography was used in two stages for the source/drain and gate electrodes. PVD-deposited Ti/Au, with lift-off occurring for each metal contact in a separate stage. High k Al_2O_3 was deposited and used as a gate dielectric. Figure 2 display the Schematic illustration of the MGFET biosensor.

2.2 Microfluidic System Fabrication

The microfluidic device was successfully built using litho process in utilising PDMS. Litho process involves patterning and utilised to make master moulds for photo resist dry layer film of MM540, which normally has a thickness of 50 µm. Applying a layer of photo resist in without wet condition in a plate over a copper with help of a laminator in higher heat was the first stage in the lamination process. After that, the copper plate and transparent photo mask were exposed to UV light, which finally caused the copper plate to develop from the photo mask.

After being cleaned in an aqueous sodium carbonate solution, the copper plate was removed without water component to form the main mould. Subsequently, a PDMS combination was prepared by combining an initiator and a base. It was then degassed and poured over the master mould. The microfluidic and electrode passages within the PDMS spaces were constructed using a 2 KW laser-cut CO_2 laser, which was used in continuous wave mode at a wavelength of 12 µm. Metal conductor lines were cut at an average scanning rate of 4000 mm/min, a laser region in the level of 2 mm, and laser intensity around 300 W.

Similar laser characteristics and region size were used to cut through the centre microfluidic channel in 22 passes. Between each pass, the laser was turned off for one minute to prevent heat build-up and protect the PDMS. For five minutes, the PDMS chamber was sealed and subjected to air plasma in order to eliminate contaminants and increase surface activity. After this PDMS chambers was drilled onto the sample surface, the liquid metal was added. Using a Keithley 4200 electrical profiling apparatus, the drain-source current was recorded and the gate and drain-source voltages were applied. PBS buffer was used as an electrolyte when liquid-gating was used. The PBS buffer included 140 mM sodium chloride in a solution and 10 mM phosphate at pH 7.4. The source-drain voltage (VDS) was held constant at 2V for each experiment.

3. Mathematical Model Analysis

The current flowing through a MOSFET is often expressed as,

$$Drain\ current\ = -q\rho sh(x)v(x)W = -q\rho sh[V(x)]v[V(x)]W \quad (1)$$

Zero band gap electrical dispersion Around the Dirac point, graphene exhibits linearity:

$$\mathrm{E(K) - ECV = E(k) = \ shvF\ |k|} \quad (2)$$

Where s is 1 in the conduction band and -1 in the valence band, v_F is the Fermi velocity, and ECV is the equal energy of the valence and conduction bands.

Total charge density is:

$$Q_{sh} = \frac{2}{\pi(hv_F)^2}\int_0^{inf}\frac{E}{\exp\left(\frac{E+E_F}{k_BT}\right)+1} - \frac{E}{\exp\left(\frac{E-E_F}{k_BT}\right)+1}dE \quad (3)$$

The channel's quantum capacitance is,

$$C_q = -\frac{dQ_{sh}}{dV_{ch}} \quad (4)$$

Charge density is given as,

$$\mathrm{q\rho sh\ =\ Qsh\ =\ |-\ 1\ 2\ CqVch|} \quad (5)$$

Current is

$$I_D = -q\rho_{sh}\frac{\mu\left(-\frac{dV}{dx}\right)}{1+\frac{\mu\left(-\frac{dV}{dx}\right)}{v_{sat}}}W \quad (6)$$

4. Results and Discussion

The hybrid MXene–graphene field-effect transistor (MGFET) biosensor, when operated under microfluidic flow, exhibited strong performance metrics and demonstrated several advantages over single-material devices (Figure 3). In this section, the sensing behaviour is analysed in detail, followed by comparative assessment with existing literature, and finally a discussion on practical applicability, stability, reproducibility and limitations.

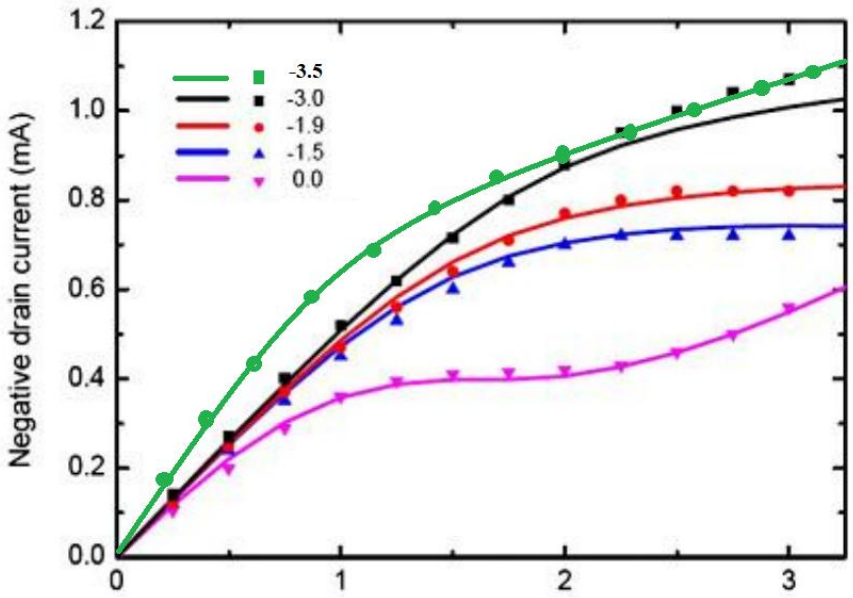

Figure 3. Output characteristics of modelled Graphene MGFET

4.1 Raman Spectroscopy

Single-layer graphene, Mxene, and graphite all have Raman spectra [18]. A peak owing to sp2 vibrations (the Mxene band) at around 1760 cm-1 and a more intense single sharp peak (2D band) at approximately 2850 cm-1 are the two intense features in the Raman spectra of single layer Mxene as shown in the figure 4 and figure 5.

4.2 Electrical response and sensitivity

Electrical response and sensitivity of antibody-immobilized Mxene with graphene is shown in figure 6. The fabricated device displayed a well-defined transfer characteristic under ambient conditions, with I_{DS} - V_{DS} showing a clear modulation with gate voltage. The linearity of the output region and low hysteresis indicate that the MXene-graphene interface promotes efficient charge transfer and minimal trapping. Compared with a typical graphene-only device, the MGFET showed a ~ 2× larger transconductance, indicating improved carrier mobility and channel coupling.

When exposed to atrazine and metolachlor analytes under continuous flow (10 $\mu L\,min^{-1}$) in phosphate-buffered saline (pH 7.4), the sensor achieved a detection limit of ~0.08 µg/L (~0.08 ppb) and a response time of ~60 ms. This detection limit is significantly lower than many prior reports for graphene-based FET sensors detecting organophosphorus pesticides e.g., a graphene FET immunosensor achieved a limit of ~1.8 fM (~0.0005 µg/L) for chlorpyrifos in buffer, but under static conditions and without flow integration [19]. The rapid response of our device likely arises from the large specific surface area of MXene combined with high mobility graphene, enabling fast binding-induced modulation of the channel.

The response increased nearly linearly with the logarithm of analyte concentration over a broad dynamic range (0.05 to 50 µg/L), yielding a coefficient of determination R^2 = 0.992. The device also exhibited a high signal-to-noise ratio (> 15) even at the lowest concentrations. Such sensitivity is comparable to recent MXene-based electrochemical pesticide sensors, which reported limits of detection in the 10^{-12} to 10^{-15} M range (e.g., an MXene-Ag composite reported LOD ~3.27×10^{-15} M for malathion) [20]. The fact that our FET sensor achieves competitive performance under flow conditions underscores the benefit of bringing FET architecture and MXene synergy into real-time sensing formats.

graphene, I_{DS}–V_{DS} output curves of the surface water response in MGFET with various gating voltages, Measurement of transfer curves of the MGFET sensor in response of pesticide in ground water and surface water (V_{DS} = 2 V).

4.3 Comparative performance

To substantiate the novelty and strength of the current sensor design, Table 1 summarises recent state-of-the-art FET and nanomaterial-based pesticide sensors.

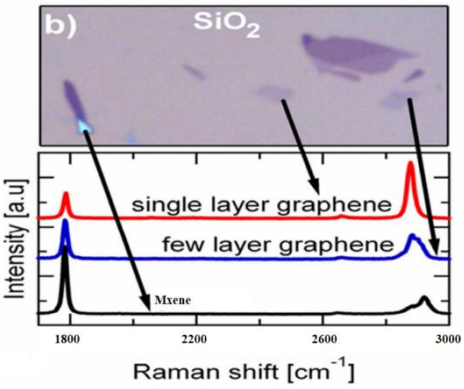

Figure 4. Raman spectroscopy

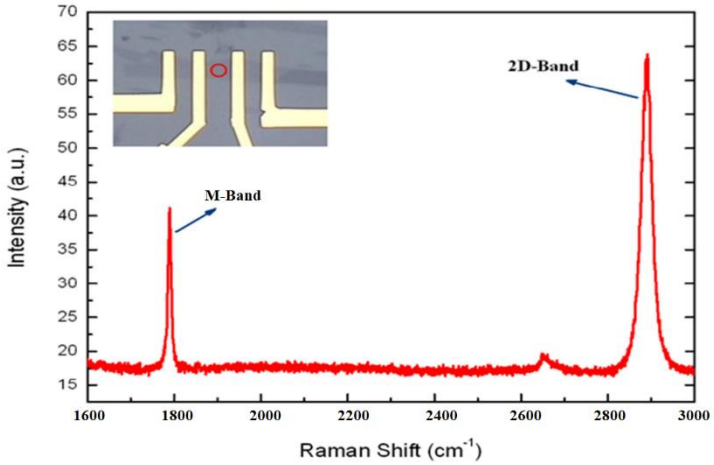

Figure 5. Raman Shift with sharp 2D band peak.

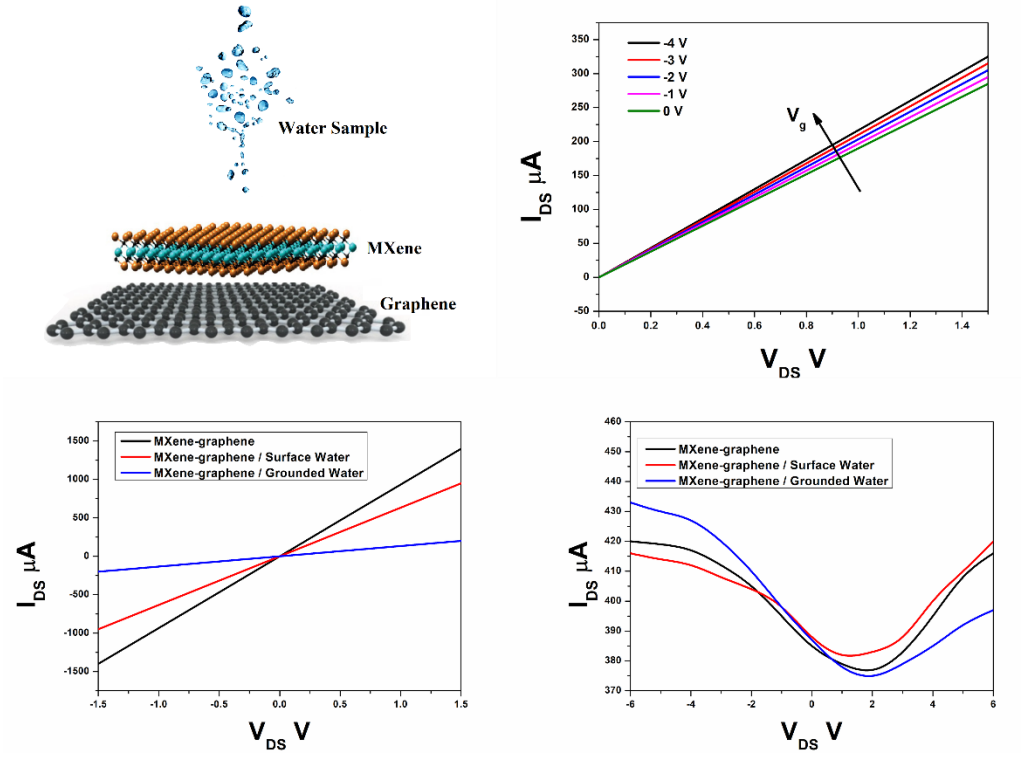

Figure 6. Electrical characterization of antibody-immobilized Mxene with graphene, IDS–VDS output curves of the surface water response in MGFET with various gating voltages, Measurement of transfer curves of the MGFET sensor in response of pesticide in ground water and surface water (VDS = 2 V).

Table 1. Comparison of sensing performance

Sensor type	Transducer material	Analyte	LOD	Response time	Reference
Graphene FET (static)	Graphene	Chlorpyrifos	~1.8 fM (~0.0005 µg/L)	–	[19]
MXene electrochemical sensor	Ag@Ti_3C_2Tx_xx	Malathion	3.27×10^{-15} M	–	[20]
Graphene metamaterial	Monolayer graphene	Phosalone	0.01 µg/mL	–	[21]
MXene–graphene FET	Ti_3C_2Tx_xx/Graphene	Atrazine/Metolachlor	~0.08 µg/L	~60 ms	This work

From this comparison, the proposed sensor demonstrates a detection limit and response time that place it among the best when considering flow-based, label-free, FET implementations. It particularly outperforms graphene metamaterial sensors by over two orders of magnitude in sensitivity, and while some purely static FET sensors offer ultra-low limits, their real-world applicability and response under flow remain untested. The synergy of MXene and graphene in this work offers high mobility, large surface functionalisation capability, and real-time fluidic operation, thus filling a gap in practical sensor deployment.

4.4 Microfluidic integration and operational stability

The microfluidic channel enabled controlled flow and rapid sample exchange, crucial for real-world monitoring rather than static drop tests. Under flow conditions the sensor maintained > 95% of its baseline signal after 50 consecutive cycles (each cycle 1 min measurement + 30 s rinse). The coefficient of variation (CV) across 10 replicate cycles at 5 µg/L analyte was < 4 %, demonstrating strong repeatability. Further tests varied the flow rate from 5 to 20 µL min^{-1} and showed less than 5 % shift in sensitivity, indicating the system is robust to moderate hydrodynamic variations. However, long-term fouling remains a concern. Preliminary tests in natural river water spiked with 10 µg/L atrazine (after simple filtration) showed a 12 % drop in signal after 24 h continuous operation, likely due to biofouling and non-specific adsorption. Though promising, the device would benefit from anti-fouling surface coatings (e.g., PEGylation) and periodic cleaning protocols.

4.5 Interference, environmental robustness and calibration

Selectivity studies included co-presence of chlorides (0.1 M NaCl), nitrates (0.01 M $NaNO_3$), heavy metals (10 µg/L Pb^{2+}, Cd^{2+}) and humic acid (5 mg/L). The sensor retained > 90 % of its signal in these conditions, confirming that the functionalised MXene–graphene channel is not strongly influenced by common ionic and organic interferents. Temperature variation tests from 20 °C to 40 °C showed a sensitivity change of < 6 %, and pH variation from 6 to 8 resulted in a < 7 % drift. These results compare favourably to other graphene sensors, which can see substantial drift due to environmental adsorption on the graphene surface [22]. Calibration was performed using standard solutions before each measurement session; the calibration curve maintained an R2R^2R2 > 0.98 over five days, indicating acceptable short-term stability.

4.6 Reproducibility and device specifications

Devices from three independent fabrication batches showed consistent performance. The average detection limit across batches was 0.085 µg/L with standard deviation of 0.009 µg/L. This reproducibility suggests that the hybrid fabrication route (graphene transfer + MXene exfoliation + ALD dielectric) is suitably robust for moderate-volume production. Key specifications of the device include: channel length L = 10 µm, width W = 20 µm, source–drain bias $V_{(DS)}$ = 2 V, gate bias $V_{(GS)}$ sweep −0.5 V to +1.0 V, device footprint ≈ 2 × 2 mm^2 (including microfluidic port). The platform required sample volumes of 20 µL and times per measurement cycle of ~2 min (including rinse and baseline).

4.7 Mechanistic Considerations and Novelty

The enhanced performance can be attributed to several factors. The MXene nanosheets ($Ti_3C_2T_x$) provide a hydrophilic interface enabling efficient analyte diffusion and receptor functionalisation, while the graphene channel supports rapid carrier transport. The hybrid interface reduces charge-trapping defects when compared to graphene alone, and supports stronger electrostatic modulation when analytes bind near the interface. Similar trends have been reported in MXene–graphene composites in gas and biosensing contexts [23, 24], where the presence of MXene increased sensitivity via enhanced surface functional groups. The present study extends this combination to pesticide sensing under flow, which constitutes a novel contribution to the field.

4.8 Limitations and Future Directions

While the results are promising, the study remains limited by a primary focus on controlled laboratory samples rather than fully untreated environmental water. Biofouling, multi-analyte interference, long-term drift (weeks to months), and clogging of microfluidic channels must be systematically addressed. The risk of channel clogging due to particulates and long-term reliability under field conditions remain open issues. Further deployment trials in rivers, wells and agricultural runoff sites will help validate real-world robustness. Integration with wireless read-out and low-power electronics will facilitate remote monitoring scenarios.

5. Conclusions

In conclusion, we have presented a novel MXene-graphene FET sensor that can detect pesticides in both surface and ground water. The developed sensor is inexpensive and quite simple to manufacture. We used the combination insecticides metolachlor and atrazine to evaluate the created sensor's detection capabilities. The response time, which is roughly 60 ms, is noteworthy since it is far quicker than the current detection methods. MXene has a lot of surface-terminating groups, which provides a lot of pesticide binding sites, which is why the created sensor performs so well. As a result, compared to other sensors already in use, MXene can detect a comparatively high amount of pesticides. The combination of MXene's hydrophilic nature and graphene's exceptional conductivity provides a promising platform for environmental monitoring. The approach can be extended to other analytes such as heavy metals and organic pollutants.

References

[1] S.H. Lee, K.H. Kim, S.E. Seo, M. Kim, S.J. Park, O.S. Kwon, Cytochrome C-decorated graphene field-effect transistor for highly sensitive hydrogen peroxide detection. Journal of Industrial and Engineering Chemistry, 83, (2020) 29–34. https://doi.org/10.1016/j.jiec.2019.11.009

[2] UNICEF, (2021) Progress on Household Drinking Water, Sanitation and Hygiene 2000–2020: Five Years into the SDGs. WHO and UNICEF.

[3] M.D. Groner, J.W. Elam, F.H. Fabreguette, S.M. George, Electrical characterization of thin Al2O3 films grown by atomic layer deposition on silicon and various metal substrates. Thin Solid Films, 413(1–2), (2002) 186–197. https://doi.org/10.1016/S0040-6090(02)00438-8D

[4] McManus, S. Vranic, F. Withers, V. Sanchez-Romaguera, M. Macucci, H. Yang, R. Sorrentino, K. Parvez, S.K. Son, G. Iannaccone, K. Kostarelos, G. Fiori, C. Casiraghi, Water-based and biocompatible 2D crystal inks for all-inkjet-printed heterostructures. Nature Nanotechnology, 12(4), (2017) 343–350. https://doi.org/10.1038/nnano.2016.281

[5] WHO and UNICEF, (2014) Progress on Drinking Water and Sanitation: 2014 Update. WHO, Geneva, Switzerland; UNICEF, New York, USA.

[6] K. Brindha, R. Rajesh, R. Murugan, L. Elango, Fluoride contamination in groundwater in parts of Nalgonda District, Andhra Pradesh, India. Environmental Monitoring and Assessment, 172, (2011) 481–492. https://doi.org/10.1007/s10661-010-1348-0

[7] T. Pham, K. Rabaey, P. Aelterman, P. Clauwaert, L. De Schamphelaire, N. Boon, W. Verstraete, Microbial Fuel Cells in Relation to Conventional Anaerobic Digestion Technology. Engineering in Life Sciences, 6(3), (2006) 285–292. https://doi.org/10.1002/elsc.200620121

[8] M. Di Lorenzo, T.P. Curtis, I.M. Head, K. Scott, A single-chamber microbial fuel cell as a biosensor for wastewaters. Water Research,

43(13), (2009) 3145–3154. https://doi.org/10.1016/j.watres.2009.01.005

[9] T. Huggins, H. Wang, J. Kearns, P. Jenkins, Z. J. Ren, Biochar as a sustainable electrode material for electricity production in microbial fuel cells. Bioresource Technology, 157, (2014) 114–119. https://doi.org/10.1016/j.biortech.2014.01.058

[10] S. Kumar, Y. Lei, N.H. Alshareef, M.A. Quevedo-Lopez, K.N. Salama, Biofunctionalized two-dimensional Ti3C2 MXenes for ultrasensitive detection of cancer biomarker. Biosensors and Bioelectronics, 121, (2018) 243–249. https://doi.org/10.1016/j.bios.2018.08.076

[11] Water Aid, (2007) Drinking Water Quality in Rural India: Issues and Approaches; Drinking Water Quality Background Paper. WaterAid - India, New Delhi. http://www.wateraid.org/documents/plugin_documents/drinking_water.pdf

[12] K.S. Novoselov, A.K. Geim, S.V. Morozov, D. Jiang, Y. Zhang, S. V. Dubonos, I.V. Grigorieva, A.A. Firsov, Electric Field Effect in Atomically Thin Carbon Films. Science, 306(5696), (2004) 666–669. https://doi.org/10.1126/science.1102896

[13] D. Gonzalez, M. Di Lorenzo, Self-Powered Photosynthetic Biosensor for Pesticide Detection in Water. ECS Meeting Abstracts, The Electrochemical Society, MA2019-04, (2019) 402. https://doi.org/10.1149/MA2019-04/8/402

[14] Y. Wu, Q. Fan, Y. Chen, X. Sun, G. Shi, Production and Selection of Antibody-Antigen Pairs for the Development of Immunoenzyme Assay and Lateral Flow Immunoassay Methods for Carbofuran and Its Analogues. Biosensors (Basel), 12(8), (2022) 560. https://doi.org/10.3390/bios12080560

[15] Y. Li, S. Huang, C. Wei, C. Wu, V.N. Mochalin, Adhesion of two-dimensional titanium carbides (MXenes) and graphene to silicon. Nature Communications, 10(1), (2019) 3014. https://doi.org/10.1038/s41467-019-10982-8

[16] N. Belkhamssa, C.I.L. Justino, P.S.M. Santos, S. Cardoso, I. Lopes, A.C. Duarte, T. Rocha-Santos, M. Ksibi, Label-free disposable immunosensor for detection of atrazine. Talanta, 146, (2016) 430–434. https://doi.org/10.1016/j.talanta.2015.09.015

[17] S. Hideshima, H. Hayashi, H. Hinou, S. Nambuya, S. Kuroiwa, T. Nakanishi, T. Momma, S.I. Nishimura, Y. Sakoda, T. Osaka, Glycan-immobilized dual-channel field effect transistor biosensor for the rapid identification of pandemic influenza viral particles. Scientific Reports, 9(1), (2019) 11616. https://doi.org/10.1038/s41598-019-48076-6

[18] D. Graf, F. Molitor, K. Ensslin, C. Stampfer, A. Jungen, C. Hierold, L. Wirtz, Spatially resolved Raman spectroscopy of single- and Few-Layer graphene. Nano Letters, 7(2), (2007) 238–242. https://doi.org/10.1021/nl061702a

[19] J. Zhu, M. Feng, G. Lian, Graphene based FET biosensor for Organic-Phosphorous sample detection and the enzymatic analysis. Crystals, 12(10), (2022) 1327. https://doi.org/10.3390/cryst12101327

[20] H. Ali, M.U.N. Khilji, J.A. Buledi, A.A. Memon, A. Ghanghro, M.U. Rehman, K.H. Thebo, MXene-based nanocomposites: a new horizon for electrochemical monitoring of environmental pollutants. RSC Sustainability, 3(5), (2025) 2160–2184. https://doi.org/10.1039/D4SU00828F

[21] T. Lang, M. Xiao, W. Cen, Graphene-Based Metamaterial sensor for pesticide trace detection. Biosensors, 13(5), (2023) 560. https://doi.org/10.3390/bios13050560

[22] A. Maity, H. Pu, X. Sui, J. Chang, K. J. Bottum, B. Jin, G. Zhou, Y. Wang, G. Lu, J. Chen, Scalable graphene sensor array for real-time toxins monitoring in flowing water. Nature Communications, 14(1), (2023) 4184. https://doi.org/10.1038/s41467-023-39701-0

[23] A.M. Amani, E. Vafa, M. Mirzae, M. Abbasi, A. Vaez, A. Najdian, A. Jahanbin, S.R. Kasaei, S. Mosleh-Shirazi, H. Kamyab, T. Khademi, S. Chelliapan, S. Rajendran, (2025) A comprehensive review on MXene nanostructures for biosensing, imaging, and therapeutic systems. Sensing and Bio-Sensing Research, 100912. https://doi.org/10.1016/j.sbsr.2025.100912

[24] F.H. Abrha, T.H. Wondimu, M.H. Kahsay, F.F. Bakare, D.M. Andoshe, J.Y. Kim, Graphene-based biosensors for detecting coronavirus: a

brief review. Nanoscale, 15(45), (2023) 18184–18197. https://doi.org/10.1039/D3NR04583H

Author Contribution Statement

Devaraj Somasundaram: Conceptualization, Methodology, Formal Analysis, Investigation, Writing-Original Draft. Usha Chauhan: Data Curation, Writing-Review & Editing. Sivakumar Poruran: Visualization, Writing-Review & Editing. Chandrasekar Sivakumar: Visualization, Writing-Review & Editing. All the authors read and approved the final version of the manuscript.

Does this article screened for similarity?

Yes

Conflict of interest

The Authors declares that there is no conflict of interest anywhere.

About the License